

Development of 3-foot Jumping and Walking Robot

Zhi-Ren Chen, and Pei-Chun Lin, Department of Mechanical Engineering, National Taiwan University

Abstract—This research designed a 3-foot robot that can jump and walk. A new linkage set and spring release mechanism make these two motions. Furthermore, this research builds a dynamic model to estimate the jumping behavior, and the simulation matches the test result.

Index Terms—gait generate, hybrid robot, jumping robot, linkage, tripedal

I. INTRODUCTION

In recent decades, there has been much research in bionic robots, but the main research aspects are the walking robots like bipeds, quadrupeds, etc. The research on robots with jumping behavior is relatively few. Furthermore, most creatures have multiple motions, but a robot with two or more motions is rare. So this research will focus on a robot with jumping and walking movements.

There have many ways to make the robot jump, like spring[1] and pneumatic[2][3]. To make the robot smaller, choose the spring as the jumping force because pneumatic requires a larger area. Many robots use linkage to convert the spring force into the desired direction[4]. So this research also uses linkage to make the robot jump and add a crank to make the robot have a walking gait.

II. FOOT LINKAGE DESIGNON

The robot's foot is a 7-bar linkage with 2 degrees of freedom. This linkage set can provide two different modes: jumping(Fig. 1) and walking(Fig. 2).

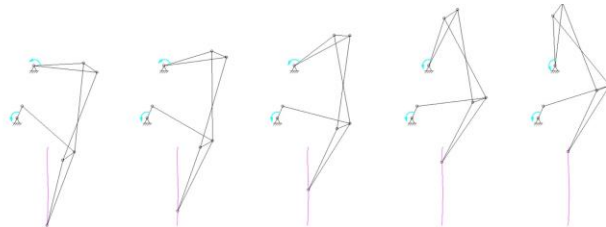


Fig. 1. The jumping motion.

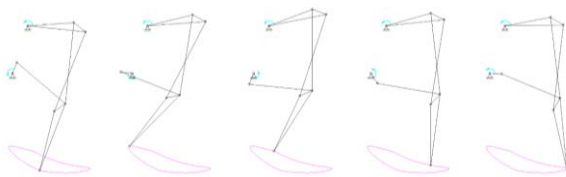


Fig. 2. The walking motion.

This work is supported by Ministry of Science and Technology (MoST), Taiwan, under contract: MOST 110-2221-E-002-111-MY3.

The authors are with Department of Mechanical Engineering, National Taiwan University (NTU), No.1 Roosevelt Rd. Sec.4, Taipei 106, Taiwan. (Corresponding email: peichunlin@ntu.edu.tw).

In jumping mode, the tiptoe will move straight when the upper linkage moves while the lower crankshaft fixes. The slope of the tiptoe track changes when the lower crankshaft is fixed in a different location, giving the jumping motion more mobility. In walking mode, the foot will provide a walking gait when the upper linkage and lower crankshaft are both moving.

III. ROBOT DESIGN

After determining the linkage parameter, next is designing the single-foot mechanism. The linkage needs to move very fast while jumping, but the motor cannot produce massive torque and high speed at the same time. So the robot stores energy in the spring. And using some mechanism to release the energy.

A. Design Generation 1

Use a cam to drive the linkage. Also, connect the motor and the linkage using a non-circular gear set so that the motor can run faster when the spring compression is low and have more torque when the spring compression is high.

However, the calculation of the non-circular gear is complicated, and it is not suitable for transmitting high torque during the actual test. In addition, the cam mechanism requires a larger space, the body design is relatively hard, and there are also some strength problems.

B. Design Generation 2

The second-generation design refers to the escapement mechanism of the ball-type bouncing robot[5]. This mechanism can use one motor to complete the function of storing elastic force and releasing it. The mechanism consists of a set of incomplete gears and a set of ratchets. The incomplete gear connects to the motor and the pawl, linked with a one-way bearing.

So when the motor is activated, it will drive the connecting rod to tighten the spring. The pawl will not release because the drive shaft and the pawl are linked with a one-way bearing.

Because of the one-way bearing, the motor can rotate in the opposite direction when the missing tooth gear does not mesh with the output gear. The pawl is released, freeing the stored force of the spring.

C. Design Generation 3

The mechanism is simplified, with only a set of missing gears driving the connecting rod in the third-generation design. That means the released elastic force is fixed, and the gear modulus is increased to 0.8 to strengthen the gear's strength; In addition, the connecting rod is strengthened. The connecting rod will rotate 100° and release the elastic stress since there are 36 teeth on the linkage gears and 10 teeth on the incomplete gear (the reduction ratio is 2.25).

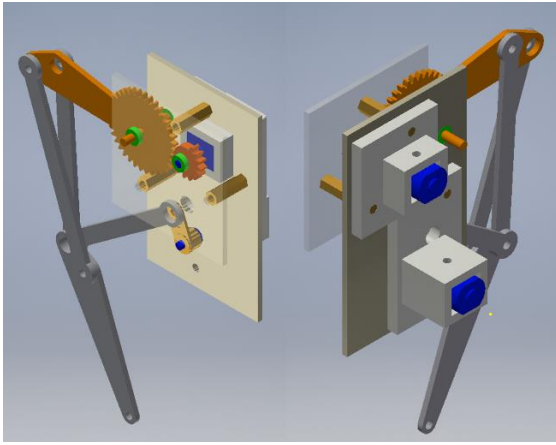


Fig. 3. The design generation 3.

The finished prototype is shown in Fig. 4. Due to a lack of space and interference issues, the spring connects to a cantilever. Using a perforated plate, determine the best position for the spring installation. The connecting rod has a hole to install a magnet to detect the location. During the test, the connecting rod would break easily. So new connecting rods are designed to improve the strength. There were also brackets for adding Hall sensors, motor control boards, and wires.

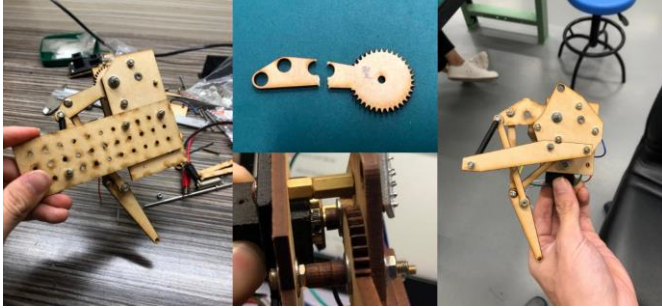


Fig. 4. The robot prototype.

C. Body Design

Each foot is an independent module for ease of design and assembly. CAD software calculates the relative distance between each module, and then the hexagonal copper column is utilized to connect each module. Change the material to an acrylic plate, give durability, and more convenience for wiring and maintenance.

Furthermore, the front and rear foot modules are not connected parallel. Because the robot is not very stable when walking during testing. There is an angle between the front and rear foot modules to lower the center of gravity and correct the walking gait. After trial and error, the front and rear foot modules are at a 19-degree angle.

IV. THE CONTROL SYSTEM

To provide higher torque and less weight the power source is an N20 DC motor with a 380 reduction ratio gearbox, and the torque is about 2.5kg·cm; each N20 has an encoder with 14 pulses per revolution. So one rotation of the output shaft will generate 5320 pulses. The N20 is controlled by the L9110 and connected with an external 9V power supply.

The controller is NI myRIO from National Instruments, driven by the LabVIEW, and provides power for the encoder

and Hall sensor. The wiring diagram of the robot is shown in Fig. 5.

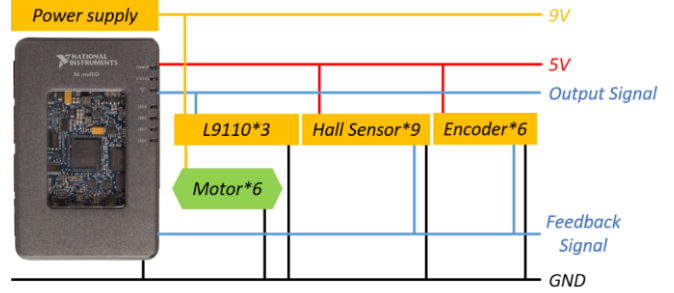


Fig. 5. The wiring diagram of the robot.

The NI myRIO and battery are relatively heavy compared to the robot, so the NI myRIO and power supply are not on the robot, replacing the battery with the power supply.

To make testing the robot and wiring more convenient, a circuit board with a male socket for NI myRIO can group the pins first, and using flat cables connect to the various modules of the robot, making the wiring tidier.

In addition, a shelf to support the cable prevents the cable from interfering with the robot dynamics. Fig. 6 shows the actual test method of the robot and the design of the male circuit board.

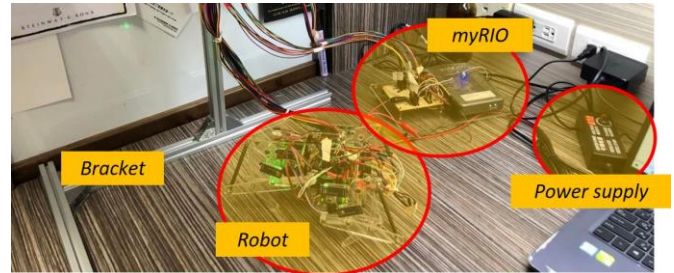


Fig. 6. The robot testing system.

V. THE DYNAMIC MODEL

A. The Robot Moment of Inertia and Elastic Coefficient

Because the feet of the robot are all on a two-dimensional plane, the robot only rotates in the roll and pitch directions when jumping.

Therefore, the moment of inertia of the robot in these two directions is measured. Use the torsional pendulum to measure the moment of inertia of the robot. Through a simple device, fix the axis of the robot at the center of the suspension point, and then let the robot rotate in the direction of roll and pitch, calculate its rotation period and measure other parameters, and then calculate the moment of inertia with the following formula:

$$J = \frac{mgRr}{\omega_n^2 H} \quad (1)$$

Among them, m is the mass of the robot (538g), g is the gravitational acceleration constant, R and r are the radii of the circle formed by the upper and lower suspension points respectively, and ω_n is the rotation frequency of the suspended object when it rotates, and H is the height difference between the suspension points.

After calculation, the moment of inertia in the roll direction is 0.1725 kg·m², and the moment of inertia in the pitch direction is 0.1682 kg·m².

Because the actual performance of the motor may differ from the information provided by the manufacturer, the spring selection method is to try many springs with similar lengths but different elastic coefficients to find the most suitable spring. The elastic coefficient is about 5.94 g/mm, but about 190 g of preload is required to get the spring to start to stretch.

.B. The Linkage System Simplification

Because the dynamics of the connecting rod are very complex, the entire system of the connecting rod and the spring is simplified as a nonlinear spring, and the direction of the force can also change. Fig. 7 shows the motion trajectory of the tiptoe under different initial conditions, when the lower link rotates to the left from the initial point, the trajectory is almost a vertical line, so when the lower link is rotated to the left, regarded as a vertical spring, but the placement position is different; when turning right, the slope of the linear motion begins to decrease as the offset increases.

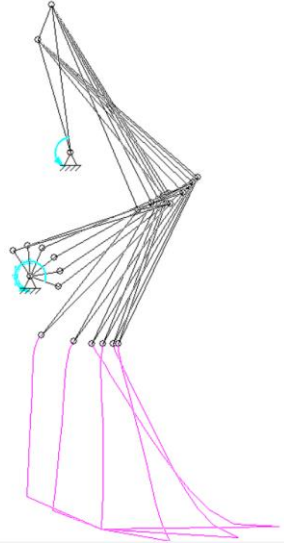


Fig. 7. The tiptoe trajectories under different initial conditions.

The following will discuss five offsets: -0.5rad, -1rad, -1.5rad, 0.5rad, and 1rad. Fig. 8 represents the force stored by the spring when the foot link retracts. The vertical axis of the picture is the upper connection. When the rod is at different angles, the elastic force provided by the spring, the horizontal axis is the angle of the upper link into the displacement of the foot. Under different initial conditions of the lower link, the relative relationship between the displacement and the elastic force is very close to linear. For the convenience of calculation, the following assumes that the entire foot system is a linear spring.

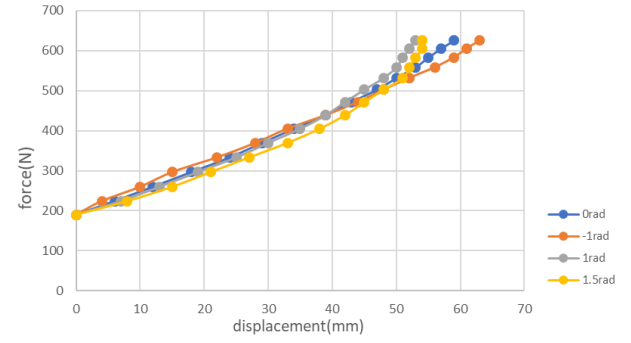


Fig. 8. Force reaction under different initial conditions.

TABLE I. shows the foot trajectories calculated by the software. The lengths of the trajectories are very close. Therefore, assumed that the connecting rod with full elastic force is a spring with a compression of 56mm, which will have different positions under different initial conditions. And the placement angle; in fact, the maximum stretch of the spring is 73.2mm, so after conversion, the elastic coefficient of the foot is 7.76 g/mm, and a pre-force of 190g is required to start stretching.

TABLE I. FOOT TRAJECTORIES UNDER DIFFERENT INITIAL CONDITIONS

| Offsets | X position (m) | Y position (m) | Slope | Stroke(mm) |
|---------|----------------|----------------|----------|------------|
| -1.5rad | 0.103 | 0.541 | -1.5 | 57.7 |
| -1.0rad | 0.110 | 0.541 | -1.8 | 59.0 |
| -0.5rad | 0.111 | 0.541 | -4.0 | 53.6 |
| 0rad | 0.107 | 0.541 | vertical | 60.0 |
| 0.5rad | 0.097 | 0.542 | vertical | 52.3 |
| 1rad | 0.087 | 0.544 | vertical | 52.2 |

.C. The Dynamic Model Calculation

The following discusses the robot dynamics when it jumps back and forth. This dynamics is related to the pitch direction and controlled by two sets of springs. Therefore, refer to the thesis [6] of I-Chia Chang to calculate the robot dynamics.

The simplified model of the robot regards the robot as a rigid body. The left and right sides of the rigid body are connected with two springs. The body moves in the yz direction, having only two degrees of freedom up and down in the z-direction, and rotating against the center of mass. A schematic diagram of the model is shown in Fig. 9:

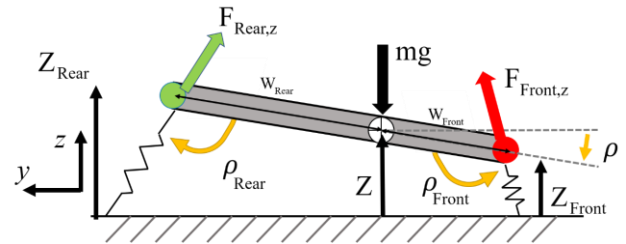


Fig. 9. The dynamic model.

Through measurement, $W_{Rear} = 91\text{mm}$, $W_{Front} = 39\text{mm}$, $J_{pitch} = 0.1682\text{ kg}\cdot\text{m}^2$ at initial conditions.

From the free body diagram in Fig. 9, ignoring the mass of the spring can give the equation for the balance of force and moment:

$$\begin{cases} F_{Rear} \sin(\rho + \rho_{Rear}) + F_{Front} \sin(\rho + \rho_{Front}) - mg = m\ddot{z} \\ F_{Rear} \sin\rho_{Rear} - F_{Front} \sin\rho_{Front} = J\ddot{\theta} \end{cases} \quad (2)$$

Because the tiptoes are close to the ground when the foot retract, assuming the length of the spring in Fig. 9 is the released length (compression amount of 56mm). According to the parameters of the spring, obtain Equation 3.(assuming the initial conditions of the two front feet are the same, So multiply by two):

$$\begin{cases} F_{Rear} = 7.76 \left(56 - \frac{W_{Rear} \sin \rho + z}{\sin(\rho + \rho_{Rear})} \right) + 190 \\ F_{Front} = 15.52 \left(56 - \frac{-W_{Front} \sin \rho + z}{\sin(-\rho + \rho_{Front})} \right) + 380 \end{cases} \quad (3)$$

Substitute Equation 2. to get the vertical displacement of the center of mass and the rotation angle of the robot.

According to TABLE I, we can know W_{Rear} , W_{Front} , ρ_{Rear} , ρ_{Front} under different initial conditions, and the results are in TABLE II:

TABLE II. W_{Rear} , W_{Front} , ρ_{Rear} UNDER DIFFERENT INITIAL CONDITIONS

| Offsets | W_{Rear} (mm) | W_{Front} (mm) | $\rho_{Front} = \rho_{Rear}$ (deg) |
|---------|-----------------|------------------|------------------------------------|
| -1.5rad | 87 | 35 | 123.7 |
| -1.0rad | 94 | 43 | 119 |
| -0.5rad | 95 | 42 | 104 |
| 0rad | 91 | 39 | 90 |
| 0.5rad | 81 | 29 | 90 |
| 1rad | 71 | 19 | 90 |

Fig. 10 shows the numerical result in which the front and rear feet are not offset ($W_{Rear}=91\text{mm}$, $W_{Front}=39\text{mm}$, $\rho_{Rear}=90\text{deg}$, $\rho_{Front}=90\text{deg}$). When x is bigger than 0.065m, the foot has fully extended, and the robot has jumped into the air. From the result, in 0.1 seconds, the robot will jump to the highest point, about 115mm high, and the rotation in the pitch direction is about 1.4 degrees, can predict that the robot's posture will be quite stable when the front and rear feet are not offset.

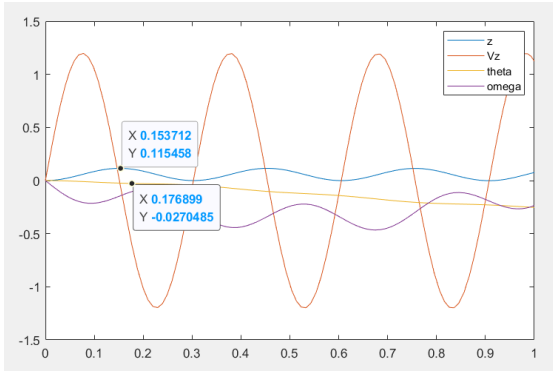


Fig. 10. The numerical result with no offset. ($W_{Rear}=91\text{mm}$, $W_{Front}=39\text{mm}$, $\rho_{Rear}=90\text{deg}$, $\rho_{Front}=90\text{deg}$)

To make the robot jump forward, change the initial conditions to provide the force in the y-direction, so set the two front feet without offset ($\rho_{Front}=90\text{deg}$), and gradually increase ρ_{Rear} to analyze the stability of the robot.

Fig. 11 is the result of the offset below the rear foot -1.5rad ($W_{Rear}=87\text{mm}$, $W_{Front}=39\text{mm}$, $\rho_{Rear}=123.7\text{deg}$, $\rho_{Front}=90\text{deg}$).

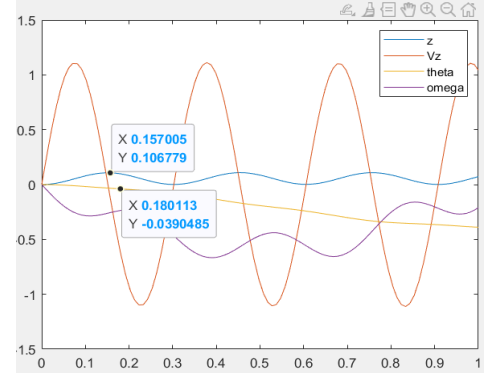


Fig. 11. The numerical result with offset. ($W_{Rear}=87\text{mm}$, $W_{Front}=39\text{mm}$, $\rho_{Rear}=123.7\text{deg}$, $\rho_{Front}=90\text{deg}$)

The rotation is not too heavy, so it can predict that the robot posture will be stable when the front and rear feet have offset.

VI. RESULT

The association between the three feet is significant. If a foot activates in advance, the robot will overturn immediately. So it is necessary to use an encoder and hall sensor at the activation point to control the release timing. In addition, wrap some clay around the robot's feet to increase the grip and prevent the tiptoe from slipping.

A. Vertical Jumping

Fig. 12 shows the jumping decomposition action of the robot (video: <https://youtu.be/IJhPbnIKLOU>)

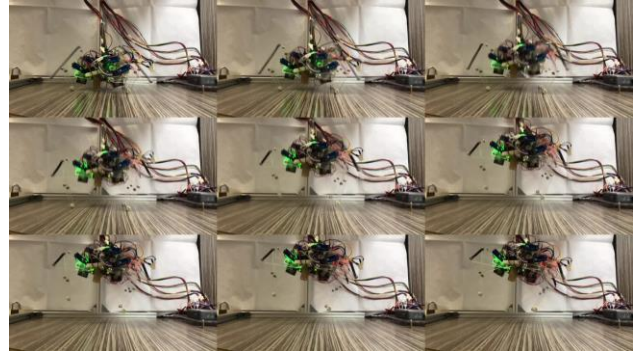


Fig. 12. The vertical jumping decomposition.

The robot's vertical jumps are very stable. Next, use Tracker to analyze the jumping height of the robot. As shown in Fig. 13, the bounce height of the robot is about 124.2mm, which is very close to the calculated 115mm. In addition, the robot trajectory is almost a straight line, the offset is only 6mm, and rotating about 10 degrees in the pitch direction.

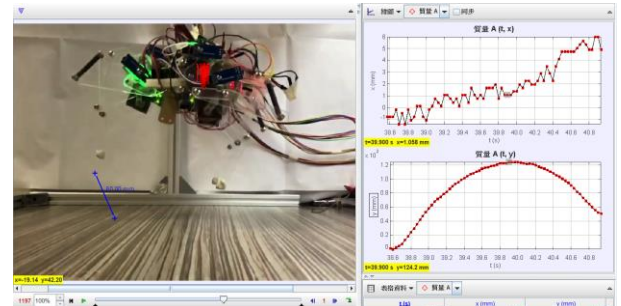


Fig. 13. Tracker analysis.

B. Jumping Forward

The forward jump test uses the initial conditions of Fig. 11. Fig. 14 shows the decomposition action of the robot jump:(video: <https://youtu.be/qN51QG4hyZM>)

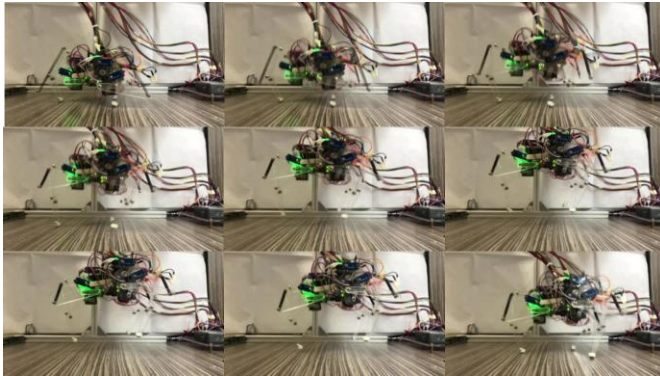


Fig. 14. The forward jumping decomposition.

The robot successfully jumps forward. Use Tracker to analyze the robot's bounce performance also. The robot's bounce height is about 107mm, which is lower than the vertical take-off height. The horizontal jump distance is 71.5mm, and the horizontal speed is about 23.6mm/s. In addition, the pitch rotation of the robot is even less than the rotation of the horizontal take-off, only about 5 degrees.

C. Walking Motion

Because the gait research of three-legged robots is relatively rare, the walking gait is through trial and error. To reduce the degree of freedom the two front feet are in the same phase, just to consider the phase of the front feet and rear feet. When the rear foot phase is 90 degrees ahead of the front foot, there will be a set of stable gaits.

Fig. 15 shows the walking decomposition of the robot (video: <https://youtu.be/2niKAjwUPw>). Interestingly, the robot will rock back and forth when walking, and the walking method is as follows:

1. When the body falls forward, the normal force of the rear foot is reduced, and it can slide forward.
2. After the back foot slides for a certain distance, the body begins to fall backward, the normal force of the rear foot increases, and the friction force also increases, so the robot will not slide backward. The normal force of the front foot decreases, it can slide forward at this time.
3. After the front foot slides for a certain distance, the robot starts to fall forward and returns to the state of 1.

According to Tracker, the walking speed of the robot is about 12.3mm/s

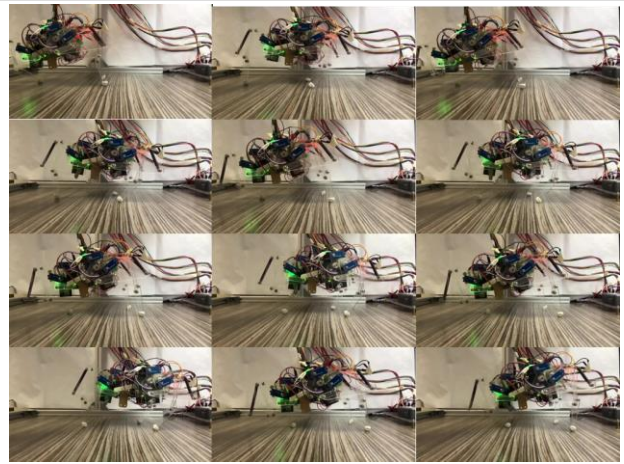


Fig. 15. The walking motion decomposition.

ACKNOWLEDGMENT

The work is supported by College Student Research from Ministry of Science and Technology (MoST). And I am very grateful to Professor Pei-Chun Lin for his guidance.

REFERENCES

- [1] Guifu Luo, Ruilong Du, Shiqiang Zhu, Sumian Song, Haihui Yuan, Hua Zhou1, Minguo Zhao and Jason Gu "Design and Dynamic Analysis of a Compliant Leg Configuration towards the Biped Robot's Spring-Like Walking" *Journal of Intelligent & Robotic Systems* (2022)
- [2] Koh Hosoda, Yuki Sakaguchi, Hitoshi Takayama and Takashi Takuma, "Pneumatic-driven jumping robot with anthropomorphic muscular skeleton structure" *Auton Robot* (2010)
- [3] Xiangxiao Liu, Yu Duan, Arne Hitzmann, Yuntong Xu, Tsungyuan Chen, Shuhei Ikemoto and Koh Hosoda1, "Using the foot windlass mechanism for jumping higher: A study on bipedal robot jumping" *Robotics and Autonomous Systems* 110 (2018)
- [4] Long Bai1, Wenjie Ge1, Xiaohong Chen1 and Ruifeng Chen, "Design and Dynamics Analysis of a Bio-inspired Intermittent Hopping Robot for Planetary Surface Exploration" *International Journal of Advanced Robotic Systems*
- [5] Bing Li, Qiang Deng and Zhichao Liu "A spherical hopping robot for exploration in complex environments" *2009 IEEE International Conference on Robotics and Biomimetics (ROBIO)*
- [6] I-Chia Chang, Chih-Hsiang Hsu, Chih-Hsiang Hsu and Pei-Chun Lin, "An analysis of the rolling dynamics of a hexapod robot using a three-dimensional rolling template" *Nonlinear Dynamics*